



Experimental demonstration of tunable de-aggregation from 16-QAM to 4-PAM for two wavelength multiplexed channels using wave mixing in a single nonlinear element to map constellation onto axes

Ahmad Fallahpour^{a,*}, Fatemeh Alishahi^a, Yinwen Cao^a, Amirhossein Mohajerin-Ariaei^a, Ahmed Almainan^{a,b}, Peicheng Liao^a, Changjing Bao^a, Morteza Ziyadi^a, Bishara Shamee^a, Joseph Touch^c, Moshe Tur^d, Alan E. Willner^a

^a Department of Electrical Engineering, University of Southern California, Los Angeles, CA 90089, USA

^b King Saud University, Riyadh, Saudi Arabia

^c Independent Consultant, Manhattan Beach, CA 90266, USA

^d School of Electrical Engineering, Tel Aviv University, Ramat Aviv 69978, Israel

ARTICLE INFO

Keywords:

Optical de-aggregation
Nonlinear wave mixing
Highly nonlinear fiber

ABSTRACT

We experimentally demonstrate tunable de-aggregation of two data carrying optical channels using nonlinear wave mixing. For each channel, the signal and its conjugate are coherently added and subtracted in order to map the constellation points onto real and imaginary axes, respectively. Each of two 10 and 15 Gbaud optical channels with a format of 16-quadrature amplitude modulation (16-QAM) are de-aggregated into two 4-level pulse amplitude modulation (4-PAM) signals. We use the same technique to de-aggregate quadrature phase shift keying (QPSK) signals into two binary phase shift keying (BPSK) signals at baud rates of 10 and 15 Gbaud for both channels. System performance is evaluated in terms of the optical signal-to-noise ratio (OSNR), and penalty of ~ 0.7 dB is observed at bit error rate (BER) of 10^{-3} .

1. Introduction

Future flexible optical networks that are heterogeneous and reconfigurable may contain various subnetworks that can have different modulation formats and spectral efficiencies. In this context, optical gateways that can convert physical layer properties from one subnetwork and make it suitable for another one might be useful. One potentially important function of such an interface would be all-optical modulation-format conversion that can avoid inefficient optical-to-electrical-optical conversion, and might enable enhanced network performance [1,2].

Potential functions at network access points include data-channel aggregation and de-aggregation in order to optimize spectral usage. By aggregating multiple data-channels of lower-order modulation formats into a single higher order one, spectral efficiency in terms of bit/s/Hz would increase. Aggregation can be implemented by nonlinear wave mixing of multiple lower rate signals in a nonlinear element to generate the aggregated signal at the output. The concept of vector addition can be exploited to perform the aggregation of the phase locked signals. In this context, each data symbol on a constellation diagram can be represented as a vector that has both magnitude and

direction. Such optical aggregation has been demonstrated to generate 16-quadrature-amplitude-modulation (QAM) by aggregating four on-off keying (OOK) signals [3], and 64-QAM by aggregating three quadrature-phase-shift-keying (QPSK) data-channels [4].

De-aggregation, the inverse function of aggregation, is the decomposition of a single higher-order modulation format to multiple lower-order channels which has also attracted attention [5–16]. The de-aggregation of the following modulation formats have been experimentally demonstrated: (a) QPSK to binary-phase-shift-keying (BPSK) [5–8], (b) 8-PSK to 4-level pulse amplitude modulation (PAM) [9], (c) 16-QAM to 4-PAM [10–12]. Most of these approaches have employed a feedback loop to stabilize phase in the de-aggregator [5–8,11,12]. Furthermore, there have been simulations that have shown the optical de-aggregation of higher-order modulation formats: (a) 8-PSK to three BPSK signals [13], (b) 8-QAM to QPSK and amplitude-shift-keying (ASK) [14], (c) 16-QAM to two QPSK signals [15], and (d) 64-QAM to 8-PAM [16]. The previous reports [5–16] have shown the de-aggregation of a single higher-order data channel into lower-order channels. However, it might be valuable to experimentally de-aggregate

* Corresponding author.

E-mail address: fallahpo@usc.edu (A. Fallahpour).

multiple higher-order wavelength-division-multiplexed (WDM) channels simultaneously in a single nonlinear stage without the need for feedback-based phase stabilization.

In this paper, we experimentally demonstrate tunable optical de-aggregation from 16-QAM to 4-PAM for two wavelength multiplexed channels in a single nonlinear element to map constellation onto axes without the need for feedback [17]. In order to implement constellation mapping, the signal conjugate is generated and added to the signal itself. In this way, an in-phase (I) component will be produced. To generate the quadrature-phase (Q) component, we apply a 180-degree phase shift to the conjugate copy of the signal. This process can be performed concurrently for two channels on different wavelengths in a single $\chi^{(3)}$ nonlinear element. Each of two 10 and 15 Gbaud 16-QAM channels are de-aggregated to their I and Q components. Modulation format tunability is also investigated by de-aggregation of two 10 and 15 Gbaud QPSK channels into BPSK signals.

2. Concept

The concept of mapping a complex data constellation to its I and Q component is shown in Fig. 1. The I-component of the signal S is generated by adding the signal to its conjugate, i.e., $I = S + S^*$, which achieves the mapping of the constellation onto the real axis. As shown in Fig. 1, the 16-QAM signal can be de-aggregated into a 4-PAM signal on the real axis; although this signal has zero mean, it can still be called 4-PAM [9–11,16–19]. The Q-component can be derived by subtracting the signal's conjugate from itself, i.e., $Q = S - S^*$, which maps the constellation onto the imaginary axis.

The conceptual block diagram demonstrating how the mapping can be implemented in the optical domain is illustrated in Fig. 2. The first channel, $S_1(t)$, along with the two coherent pumps, $P_{11}(t)$ and $P_{12}(t)$, are coupled with another dummy pump, $P_1(t)$ into a fiber. The electric fields of the signal and the corresponding pumps can be written as follow:

$$S_1(t) = A_{S_1}(t) e^{j(\omega_{S_1} t + \varphi_{S_1}(t))} = A_{S_1}(t) e^{j(\omega_{S_1} t + \varphi_{S_1}^D(t) + \varphi_{S_1}^N(t))} \quad (1)$$

$$P_{11}(t) = A_{P_{11}} e^{j(\omega_{P_{11}} t + \varphi_{P_{11}}(t))} = A_{P_{11}} e^{j(\omega_{P_{11}} t + \varphi_{P_{11}}^N(t))} \quad (2)$$

$$P_{12}(t) = A_{P_{12}} e^{j(\omega_{P_{12}} t + \varphi_{P_{12}}(t))} = A_{P_{12}} e^{j(\omega_{P_{12}} t + \varphi_{P_{12}}^N(t))} \quad (3)$$

$$P_1(t) = A_{P_1} e^{j(\omega_{P_1} t + \varphi_{P_1}(t))} = A_{P_1} e^{j(\omega_{P_1} t + \varphi_{P_1}^N(t))} \quad (4)$$

where $A_{S_1}(t)$, $A_{P_{11}}$, $A_{P_{12}}$, and A_{P_1} are the amplitudes, ω_{S_1} , $\omega_{P_{11}}$, $\omega_{P_{12}}$, and ω_{P_1} are the wavelengths and $\varphi_{S_1}(t)$, $\varphi_{P_{11}}(t)$, $\varphi_{P_{12}}(t)$, and $\varphi_{P_1}(t)$ are the phases of $S_1(t)$, $P_{11}(t)$, $P_{12}(t)$, and $P_1(t)$, respectively. Phase of the signal include both data and noise, $\varphi_{S_1}^D(t)$ and $\varphi_{S_1}^N(t)$; however, pumps only carry the phase noises. $P_{11}(t)$ and $P_{12}(t)$ are placed in symmetry with respect to $S_1(t)$, and if the pumps and the signal are coherent, following equations can be used:

$$\omega_{P_{12}} - \omega_{S_1} = \omega_{S_1} - \omega_{P_{11}} = \Delta\omega \quad (5)$$

$$\varphi_{S_1}^N(t) = \varphi_{P_{11}}^N(t) = \varphi_{P_{12}}^N(t) \quad (6)$$

where $\Delta\omega$ is the wavelength difference between signal and its coherent pumps. A second channel, $S_2(t)$, along with two coherent pumps, $P_{21}(t)$ and $P_{22}(t)$, and a dummy pump, $P_2(t)$, can be multiplexed into the same fiber with a similar configuration to the first channel and its corresponding pumps. All signals and pumps are transmitted into a programmable filter that can adjust the amplitude and the phase of signals and pumps independently. In this filter, the complex coefficients of α and β are applied to $P_{12}(t)$ and $P_{11}(t)$, respectively. Subsequently, these signals are sent into a $\chi^{(3)}$ nonlinear material, e.g., highly nonlinear fiber (HNLF), to generate the mixing terms. In the HNLF, each three waves can mix through four-wave mixing (FWM) process under the phase-matching conditions to produce a fourth wave. Here, we focus on the generated terms that are on our wavelength of interest. Mixing of $S_1(t)$, $P_{12}(t)$, and $P_1(t)$ can generate nine new waves [20,21] including two idlers which are symmetrical with respect to $P_1(t)$. We denote the electric field of these two idlers as $X_{11}(t)$ and $X_{12}(t)$ which

are shown as follows:

$$\begin{aligned} X_{11}(t) &= P_1(t) \times S_1(t) \times \alpha P_{12}^*(t) \\ &= \alpha A_{P_1} A_{S_1}(t) A_{P_{12}} e^{j((\omega_{P_1} + \omega_{S_1} - \omega_{P_{12}})t + \varphi_{P_1}^N(t) + \varphi_{S_1}^D(t) + \varphi_{S_1}^N(t) - \varphi_{P_{12}}^N(t))} \end{aligned} \quad (7)$$

$$\begin{aligned} X_{12}(t) &= P_1(t) \times S_1^*(t) \times \alpha P_{12}(t) \\ &= \alpha A_{P_1} A_{S_1}(t) A_{P_{12}} e^{j((\omega_{P_1} - \omega_{S_1} + \omega_{P_{12}})t + \varphi_{P_1}^N(t) - \varphi_{S_1}^D(t) - \varphi_{S_1}^N(t) + \varphi_{P_{12}}^N(t))} \end{aligned} \quad (8)$$

By plugging Eqs. (5) and (6) into Eqs. (7) and (8), the latter equations can be simplified to:

$$X_{11}(t) = \alpha A_{P_1} A_{S_1}(t) A_{P_{12}} e^{j((\omega_{P_1} - \Delta\omega)t + \varphi_{P_1}^N(t) + \varphi_{S_1}^D(t))} \quad (9)$$

$$X_{12}(t) = \alpha A_{P_1} A_{S_1}(t) A_{P_{12}} e^{j((\omega_{P_1} + \Delta\omega)t + \varphi_{P_1}^N(t) - \varphi_{S_1}^D(t))} \quad (10)$$

Based on Eqs. (9) and (10) and due to the coherence between $S_1(t)$, and $P_{12}(t)$, the phase noises of the signal, $S_1(t)$, and the pump, $P_{12}(t)$, cancel each other. As a result, the phase noises of the generated idlers, $X_{11}(t)$ and $X_{12}(t)$, only depend on the phase noise of $P_1(t)$, which does not need to be phase locked to the signal. Furthermore, $S_1(t)$, $P_{11}(t)$, and $P_1(t)$ can mix through FWM and generate following electric fields:

$$\begin{aligned} X_{13}(t) &= P_1(t) \times S_1(t) \times \beta P_{11}^*(t) \\ &= \beta A_{P_1} A_{S_1}(t) A_{P_{11}} e^{j((\omega_{P_1} + \omega_{S_1} - \omega_{P_{11}})t + \varphi_{P_1}^N(t) + \varphi_{S_1}^D(t) + \varphi_{S_1}^N(t) - \varphi_{P_{11}}^N(t))} \end{aligned} \quad (11)$$

$$\begin{aligned} X_{14}(t) &= P_1(t) \times S_1^*(t) \times \beta P_{11}(t) \\ &= \beta A_{P_1} A_{S_1}(t) A_{P_{11}} e^{j((\omega_{P_1} - \omega_{S_1} + \omega_{P_{11}})t + \varphi_{P_1}^N(t) - \varphi_{S_1}^D(t) - \varphi_{S_1}^N(t) + \varphi_{P_{11}}^N(t))} \end{aligned} \quad (12)$$

By plugging Eqs. (5) and (6) into Eqs. (11) and (12), they are simplified as follow:

$$X_{13}(t) = \beta A_{P_1} A_{S_1}(t) A_{P_{11}} e^{j((\omega_{P_1} + \Delta\omega)t + \varphi_{P_1}^N(t) + \varphi_{S_1}^D(t))} \quad (13)$$

$$X_{14}(t) = \beta A_{P_1} A_{S_1}(t) A_{P_{11}} e^{j((\omega_{P_1} - \Delta\omega)t + \varphi_{P_1}^N(t) - \varphi_{S_1}^D(t))} \quad (14)$$

Similarly, $X_{13}(t)$ and $X_{14}(t)$ are symmetrical with respect to $P_1(t)$ and their phase noises only depend on the phase noise of the pump $P_1(t)$ due to the fact that $S_1(t)$ and $P_{11}(t)$ are coherent and their phase noises cancel each other.

According to Eqs. (9) and (14), $X_{11}(t)$ and $X_{14}(t)$ are phase and frequency locked; therefore, they can be coherently added as follows:

$$\begin{aligned} X_{11}(t) + X_{14}(t) &= \left(\alpha A_{P_1} A_{S_1}(t) A_{P_{12}} \right. \\ &\quad \left. + \beta A_{P_1} A_{S_1}(t) A_{P_{11}} \right) e^{j(\omega_{P_1} - \Delta\omega)t + \varphi_{P_1}^N(t)} \left(e^{j\varphi_{S_1}^D(t)} + e^{-j\varphi_{S_1}^D(t)} \right) \\ &= \left(\alpha A_{P_1} A_{S_1}(t) A_{P_{12}} \right. \\ &\quad \left. + \beta A_{P_1} A_{S_1}(t) A_{P_{11}} \right) e^{j(\omega_{P_1} - \Delta\omega)t + \varphi_{P_1}^N(t)} \left(2\cos\varphi_{S_1}^D(t) \right) \end{aligned} \quad (15)$$

Note that the coefficients α and β are adjusted such that the amplitudes of $X_{11}(t)$ and $X_{14}(t)$ to be equal. Eq. (15) indicates the constellation points that are symmetric with respect to the real axis are mapped to the same value on real axis. For example, for both $\varphi_{S_1}^D(t) = \pi/4$ and $\varphi_{S_1}^D(t) = -\pi/4$, the output is proportional to $\cos\varphi_{S_1}^D(t) = \sqrt{2}/2$. This fact confirms the concept of mapping constellation to real axis which generates the I component.

By adjusting the phase of the complex coefficient β , the quadrature selection can be performed. Eq. (15) indicates that the I component can be recovered if the phase of β is equal to zero. In order to generate the Q component, we only need to apply a 180-degree phase shift to $P_{11}(t)$ by changing the phase of β in the programmable filter. In this manner, Eq. (15) is modified to:

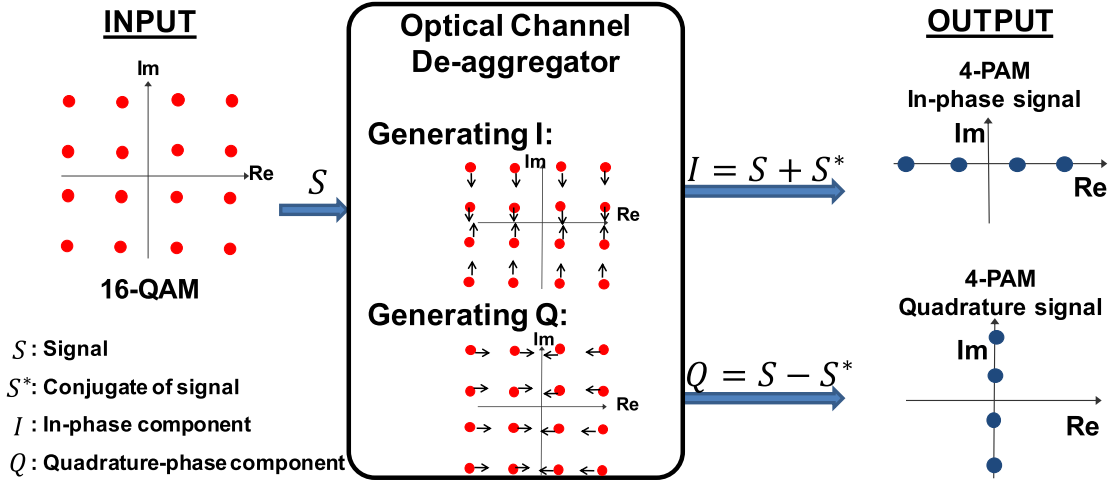


Fig. 1. Mapping 16-QAM to its I and Q components. By adding the signal with its conjugate, the I-component can be achieved. Similarly, Q-component can be generated by subtracting conjugate from the signal.

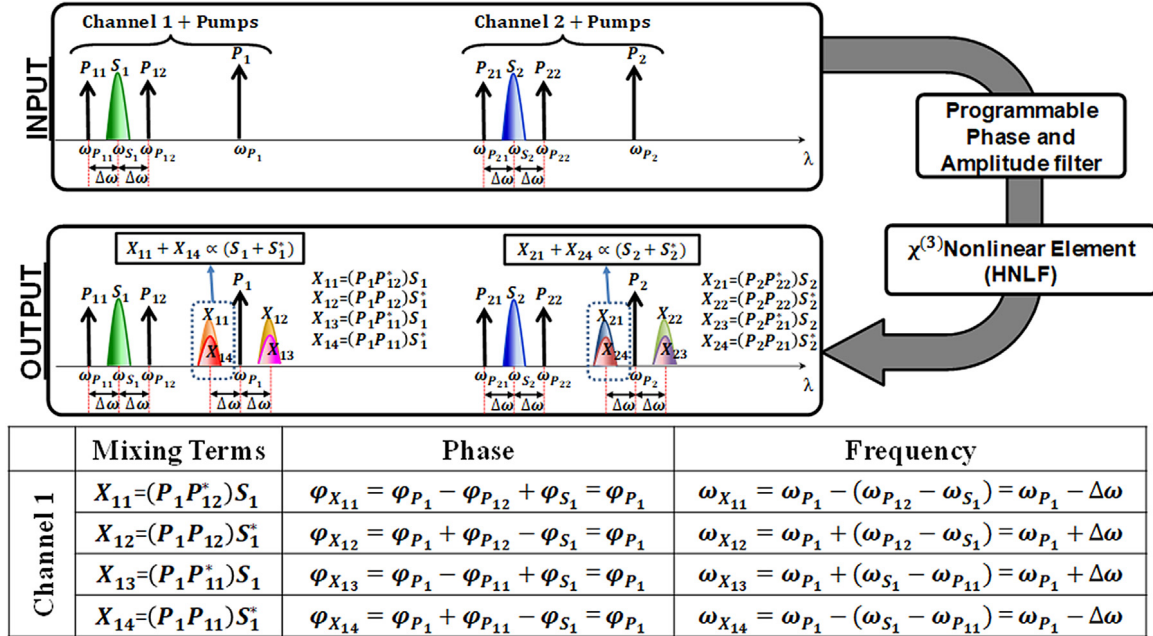


Fig. 2. The block diagram of the proposed two channel de-aggregator using mapping and wave mixing in single nonlinear stage. Signal copy and its conjugate copy are generated at the same frequency through four-wave mixing. The amplitude and phase of the signal and pumps can be adjusted in the programmable filter.

$$\begin{aligned}
& X_{11}(t) + X_{14}(t) \\
&= (\alpha A_{P_1} A_{S_1}(t) A_{P_{12}} \\
&+ \beta A_{P_1} A_{S_1}(t) A_{P_{11}}) e^{j((\omega_{P_1} - \Delta\omega)t + \varphi_{P_1}^N(t))} \left(e^{j\varphi_{S_1}^D(t)} + e^{j\pi} e^{-j\varphi_{S_1}^D(t)} \right) \\
&= (\alpha A_{P_1} A_{S_1}(t) A_{P_{12}} \\
&+ \beta A_{P_1} A_{S_1}(t) A_{P_{11}}) e^{j((\omega_{P_1} - \Delta\omega)t + \varphi_{P_1}^N(t))} \left(e^{j\varphi_{S_1}^D(t)} - e^{-j\varphi_{S_1}^D(t)} \right) \\
&= (\alpha A_{P_1} A_{S_1}(t) A_{P_{12}} \\
&+ \beta A_{P_1} A_{S_1}(t) A_{P_{11}}) e^{j((\omega_{P_1} - \Delta\omega)t + \varphi_{P_1}^N(t))} \left(2j \sin \varphi_{S_1}^D(t) \right) \\
&= (\alpha A_{P_1} A_{S_1}(t) A_{P_{12}} \\
&+ \beta A_{P_1} A_{S_1}(t) A_{P_{11}}) e^{j((\omega_{P_1} - \Delta\omega)t + \varphi_{P_1}^N(t))} e^{j\frac{\pi}{2}} \left(2 \sin \varphi_{S_1}^D(t) \right)
\end{aligned}$$

(16)

Eq. (16) shows the constellation points that are symmetric with respect to the imaginary axis are mapped to the same value on the imaginary axis. For example, for both $\varphi_{S_1}^D(t) = \pi/4$ and $\varphi_{S_1}^D(t) = 3\pi/4$, the output is proportional to $\sin \varphi_{S_1}^D(t) = \sqrt{2}/2$. Accordingly, de-aggregation of a complex constellation into the I and Q component is realized by phase adjustment of $P_{11}(t)$ and combining $X_{11}(t)$ and $X_{14}(t)$. Similarly, $X_{12}(t)$ and $X_{13}(t)$ are phase and frequency locked which can generate the de-aggregated signal at $\omega_{P_1} + \Delta\omega$. These equations can also be derived for the second channel and its corresponding pumps that lead to de-aggregation of the second channel at the HNLf output.

3. Experimental setup

The experimental setup of the proposed de-aggregator system is shown in Fig. 3(a). At the transmitter, two lasers at wavelengths of $\lambda_{S_1} = 1546.9$ nm and $\lambda_{S_2} = 1556.9$ nm are coupled into a fiber to be modulated as the first and the second channel signals. Data is

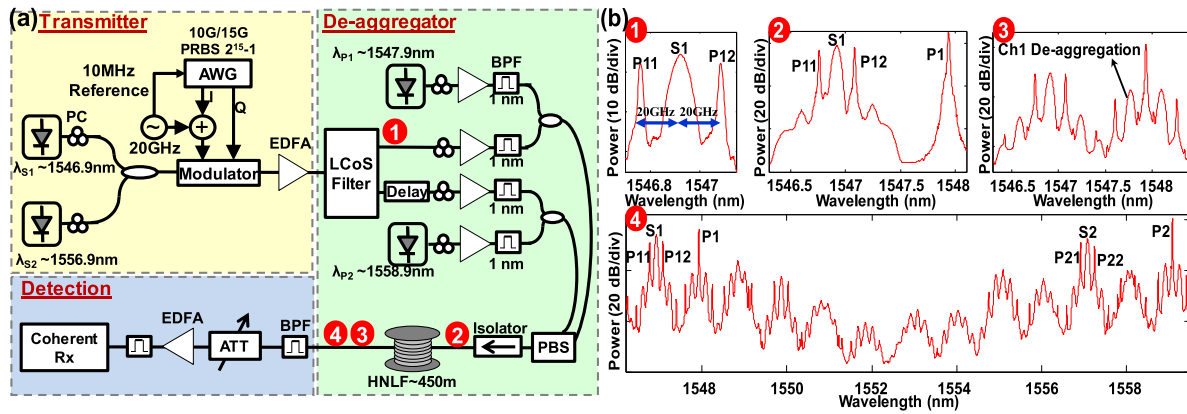


Fig. 3. (a) The experimental setup for the proposed optical channel de-aggregator; (b) the corresponding spectra measured at each node. AWG: Arbitrary Waveform Generator, EDFA: Erbium-Doped Fiber Amplifier, LCoS: Liquid Crystal on Silicon, BPF: Band Pass Filter, PC: Polarization Controller, PBS: Polarization Beam Splitter, HNLf: Highly Non-Linear Fiber, ATT: attenuator.

generated in a high-speed arbitrary waveform generator (AWG). In order to generate the coherent pumps which are symmetric with respect to the signal, the I component of the signal is mixed with a sinusoidal tone that is generated by a 20 GHz clock synthesizer. The clock in the AWG is synchronized with the synthesizer by a 10MHz reference. The spectrum of the modulated signal and its coherent pumps can be seen in Fig. 3(b1). The 20 GHz is the frequency difference between the signal and the coherent pumps ($\Delta\omega$ in Eq. (5)). By reducing the frequency difference, the spectral efficiency will be improved; however, the baud rate of the signal will be limited. In addition, by reducing the frequency of the synthesizer, the signal may experience more severe crosstalk. The amplitude of the AWG output is set ~ 250 mV peak-to-peak to keep the electrical signal at the linear region of the modulator. Moreover, the amplitude of the sinusoidal tone is tuned such that the signal and the coherent pumps have almost equal peak power (see Fig. 3(b1)).

The same data is encoded onto both channels using a nested Mach-Zehnder modulator with 10/15 Gbaud QPSK/16-QAM data generated by a $2^{15} - 1$ pseudo random bit sequence (PRBS). The output of the modulator is amplified in a low-noise erbium-doped fiber amplifier (EDFA) and sent into the optical de-aggregator. First, the signal and the pumps' amplitudes and phases are adjusted on both channels in a programmable filter based on Liquid Crystal on Silicon (LCoS) technology. Adjusting the phase of P_{11} and P_{21} in the LCoS filter can determine which quadrature will be selected at the output of de-aggregator. At the output of the filter, the two channels are decorrelated by applying delay to the second channel. Consequently, each channel is amplified to 18 dB in a high-power EDFA. Each of the laser pumps of P_1 and P_2 at wavelengths of $\lambda_{p1} = 1547.9$ nm and $\lambda_{p2} = 1558.9$ nm are also amplified in high-power EDFAs to 21 dB and coupled in to the fiber with their corresponding channels. After amplification, both channels and their corresponding pumps are combined in a polarization beam splitter (PBS) and sent into a 450 m HNLf with a zero-dispersion wavelength (ZDW) of ~ 1551 nm and a nonlinear coefficient of 20 W $^{-1}$ km $^{-1}$. The PBS could help to put two sets of waves on two orthogonal polarization before sending them into the HNLf. In this way, the nonlinear interaction between channel 1 and channel 2 could be decreased and each channel will suffer less from the mutual crosstalk. Fig. 3(b2) shows the spectrum of the first channel signal along with pumps that are arranged in the same fashion as shown in Fig. 2. The spectrum at the output of the HNLf for first channel is depicted in Fig. 3(b3). As indicated in the figure, the de-aggregated signal, which is either the I or Q component (BPSK/4-PAM) of the original signal (QPSK/16-QAM), is generated through the wave mixing described earlier. The de-aggregated signal at the output of the HNLf is filtered out by using an optical band-pass filter (BPF) and sent into an 80Gsample/s coherent receiver to be analyzed.

Fig. 3(b4) illustrates the spectrum at the output of the HNLf, including the first and the second channels, the pumps, and the de-aggregated signals for both channels. The spectrum also shows other mixing terms generated in the HNLf that are not desirable. Although these mixing terms do not impact the de-aggregated signal, they limit the number of channels that can be multiplexed for de-aggregation. This is the reason why we limit our study to two wavelength multiplexed channels.

Some of the additional undesirable mixing terms depend on the spacing between the signal and the dummy pump. In other words, if this spacing is equal for both channels, some of the generated mixing terms will overlap and they cannot be separated in the spectrum domain. In order to show all the additional mixing terms in the spectrum of Fig. 3(b4), we choose to have different frequency spacing between the signal and the dummy pump for two channels. We note that this different frequency spacing should not impact the performance of the de-aggregated signal because the additional mixing terms lie on different wavelengths.

The current setup only allows recovering one quadrature, i.e. I or Q, at a time. In order to adapt the scheme to recover two quadratures simultaneously, additional HNLf and LCoS filter should be utilized. The output of the isolator in Fig. 3(a) can be split by a 50/50 coupler into two arms to generate I and Q components simultaneously. The first arm is connected to the first HNLf to generate one of the quadratures, i.e. I or Q. The second arm can be connected to the additional LCoS filter followed by the second HNLf. In this way, the orthogonal quadrature, i.e. Q or I, can be obtained by adjusting the relative phase in the second arm using the additional LCoS filter.

4. Experiment results

Fig. 4 shows the constellations of the QPSK and 16-QAM signals at the input of the optical de-aggregator and their corresponding I and Q de-multiplexed outputs for both channels simultaneously. Two 10 Gbaud QPSK signals with error vector magnitudes (EVMS) of 11.3% and 11.8% are sent as channel 1 and 2 (respectively) and mapped onto the in-phase and quadrature-phase axes as BPSK signals with EVMS of 14.3% and 14.6% for channel 1 and 13.9% and 14.7% for channel 2. To demonstrate bitrate tunability of the proposed system, de-aggregation of a 15 Gbaud QPSK signal is also shown. Here, the EVMS of QPSK signals in channel 1 and 2 are 13.1% and 13.5%, respectively. These signals are de-aggregated into BPSK signals with EVMS of 16.7% and 16.9% for I and Q of the first channel and EVMS of 17.1% for both I and Q of the second channel. In addition, the tunability of the proposed system over the constellation is verified by changing the input constellation to 16-QAM. In channel 1, a 10 Gbaud 16-QAM signal with an EVM of 10.2% is de-multiplexed into a 4-PAM signal with an EVM of 11.4% for the I component and an EVM of 11.7% for the Q component.

		INPUT	OUTPUT	
			In-phase	Quadrature
QPSK (10 Gbaud)	Channel 1	EVM=11.3% 	EVM=14.3% 	EVM=14.6%
	Channel 2	EVM=11.8% 	EVM=13.9% 	EVM=14.7%
QPSK (15 Gbaud)	Channel 1	EVM=13.1% 	EVM=16.7% 	EVM=16.9%
	Channel 2	EVM=13.5% 	EVM=17.1% 	EVM=17.1%
16-QAM (10 Gbaud)	Channel 1	EVM=10.2% 	EVM=11.4% 	EVM=11.7%
	Channel 2	EVM=10.3% 	EVM=11.2% 	EVM=11.4%
16-QAM (15 Gbaud)	Channel 1	EVM=11.5% 	EVM=12.5% 	EVM=13.9%
	Channel 2	EVM=11.5% 	EVM=12.4% 	EVM=13.5%

Fig. 4. Constellation of the input and output of the optical channel de-aggregator. Two 10/15 Gbaud 16-QAM signals on channel 1 and 2 are de-aggregated into 4-PAM. Similarly, two 10/15 Gbaud QPSK signals are de-aggregated to BPSK for both channels.

Similarly, for channel 2, a 16-QAM signal with an EVM of 10.3% is de-aggregated into 4-PAM signals with I and Q components with EVMs of 11.2% and 11.4%, respectively. Furthermore, 15 Gbaud 16-QAM signal in channel 1 and 2 with an EVMs of 11.5% are de-aggregated to the 4-PAM signals. EVMs of I and Q components are 12.5% and 13.9% for channel 1 and they are 12.4% and 13.5% for channel 2.

The BER measurement of the optical de-aggregator is shown in Fig. 5. The BER of the 10 Gbaud QPSK signals at both channels and the de-aggregated BPSK I and Q signals at the output of two channels is plotted against the resulting optical signal-to-noise ratio (OSNR) in

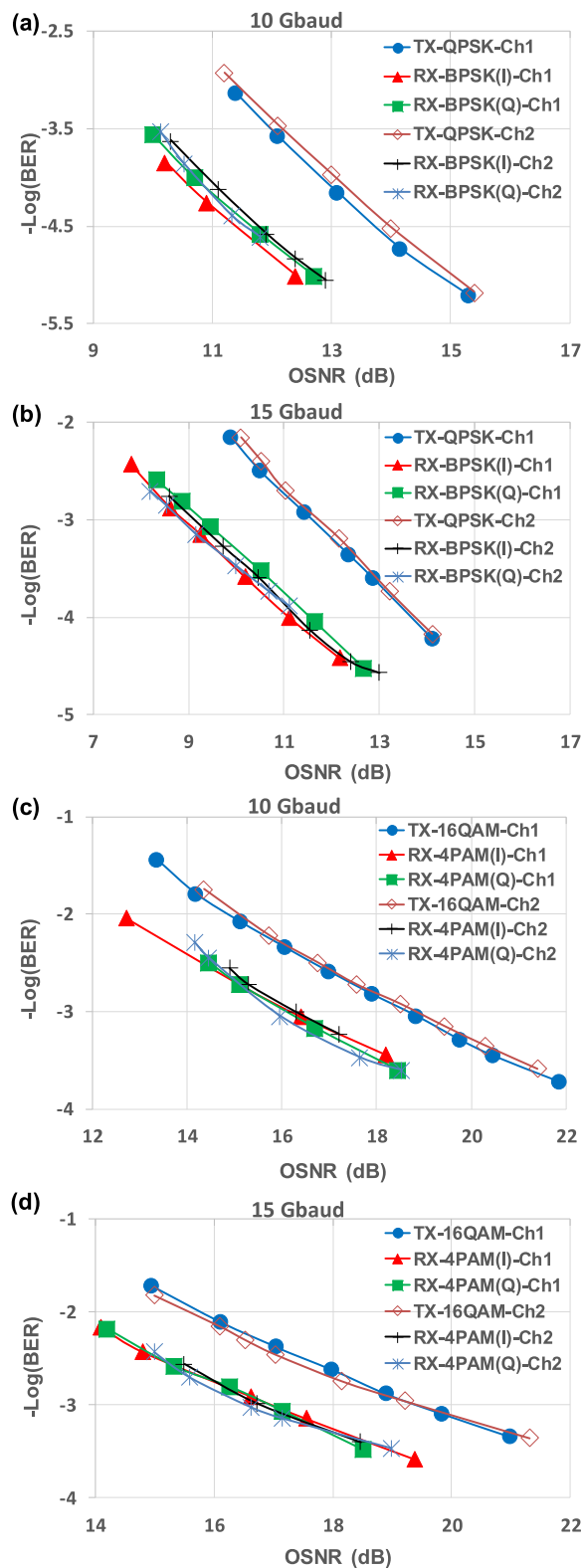


Fig. 5. BER performance of the optical de-aggregator for the input (a) 10 Gbaud QPSK, (b) 15 Gbaud QPSK, (c) 10 Gbaud 16-QAM, and (d) 15 Gbaud 16-QAM and their de-aggregated signals in both channels.

Fig. 5(a). At a BER of 10^{-4} , the OSNR difference between the input QPSK signal and the output BPSK signal is ~ 2.3 dB and ~ 2.4 dB for channels 1 and 2, respectively. Although the theoretical OSNR difference between QPSK and BPSK is 3 dB [22], the system performance is

still good, incurring a penalty of only ~ 0.7 dB. The system performance is also investigated for 15 Gbaud QPSK signals as the input of both channels. In this case, the OSNR differences are ~ 2.3 dB and ~ 2.6 dB between input and output for channels 1 and 2 at a BER of 10^{-3} . Similarly, Fig. 5(c) and (d) illustrates BER measurement for 10 and 15 Gbaud 16-QAM data channels de-aggregation into 4-PAM signals. In channel 1 the OSNR difference between 10 Gbaud 16-QAM and 4-PAM is ~ 2.3 dB and it is ~ 2.5 dB for channel 2. In 15 Gbaud case, the OSNR differences are ~ 2.5 dB and ~ 2.7 dB for channel 1 and 2, respectively, at BER of 10^{-3} . By comparing the BER of TX-QPSK and TX-16QAM with the theoretical values [23], around 6 dB penalty is observed in the experiment. This is mainly because of unoptimized DSP calculation in the coherent receiver. We did not use any equalizer at the receiver which could have improved the experimental BER performance. However, the BER of the input and the output of the experimental setup is measured under the same condition.

We note that the de-aggregated signals, i.e., BPSK and 4-PAM, are “zero mean” data streams that are similar to their original complex constellations of QPSK and 16-QAM, respectively. This means that coherent detection might be required to recover data from these signals. However, there might be interest in direct detection of the de-aggregated signals due to its simpler and less-costly implementation. One method would be to include another nonlinear stage to add a fixed amount of power to the BPSK or 4-PAM signals [24]. This enables either two-level or four-level intensity signals to be detected by direct detection. A second option is to use a delay line interferometer (DLI), which can convert multiple channels simultaneously [25]. In that case, phase information is converted into intensity by applying a one-bit delay between the two arms of interferometer. Furthermore, such formats can also be detected in two parallel direct-detection and interferometric receivers [26]. In order to optimize the performance of such a receiver, the extinction ratio of the received 4-PAM should be adjusted. However, in our scheme, the extinction ratio is dictated by the 16-QAM constellation at the transmitter.

5. Conclusion

In this paper, two channel tunable optical de-aggregator is experimentally demonstrated. The 16-QAM data channels are decomposed to their I and Q components and de-aggregated to 4-PAM signals. Similarly, QPSK signals are de-aggregated to BPSK signals. The BER measurement indicates the system penalty of ~ 0.7 dB. We also have discussed how the output of de-aggregator can be detected using direct detection.

Acknowledgment

National Science Foundation (NSF) Center for Integrated Access Networks under Grant Y501119, Huawei Technologies, The Office of Naval Research (ONR) (N000141812352).

References

- [1] A.A.M. Saleh, J.M. Simmons, All-optical networking—evolution, benefits, challenges, and future vision, *Proc. IEEE* 100 (5) (2012) 1105–1117.
- [2] A.E. Willner, A. Fallahpour, F. Alishahi, Y. Cao, A.H. Mohajerin-Ariaei, A. Almainan, P. Liao, K. Zou, A. Willner, M. Tur, All-optical signal processing techniques for flexible networks, *J. Lightwave Technol.* 37 (1) (2018) 21–35.
- [3] G. Huang, Y. Miyoshi, A. Maruta, Y. Yoshida, K. Kitayama, All-optical OOK to 16-QAM modulation format conversion employing nonlinear optical loop mirror, *J. Lightwave Technol.* 30 (9) (2012) 1342–1350.
- [4] A. Fallahpour, M. Ziyadi, A. Mohajerin-Ariaei, A. Kornds, M. Karpov, M. Pfeiffer, C. Bao, P. Liao, Y. Cao, A. Almainan, F. Alishahi, B. Shamee, L. Paraschis, M. Tur, C. Langrock, M.M. Fejer, J. Touch, T.J. Kippenberg, A.E. Willner, Experimental generation of a 64-QAM by optically aggregating three independent QPSK channels using nonlinear wave mixing of multiple Kerr comb lines, in: *Conference on Lasers and Electro-Optics*, paper JTh2A.59, 2017.
- [5] A. Lorences-Riesgo, F. Chiarello, C. Lundström, M. Karlsson, P.A. Andrekson, Experimental analysis of degenerate vector phase-sensitive amplification, *Opt. Express* 22 (18) (2014) 21889–21902.
- [6] M. Gao, T. Kurosu, K. Solis-Trapala, T. Inoue, S. Namiki, Quadrature squeezing and IQ de-multiplexing of QPSK signals by sideband-assisted dual-pump phase sensitive amplifiers, *IEICE Trans. Commun.* E98.B (11) (2015) 2227–2237.
- [7] F. Da Ros, K. Dalgaard, L. Lei, J. Xu, C. Peucheret, QPSK-To-2x4Bpsk wavelength and modulation format conversion through phase-sensitive four-wave mixing in a highly nonlinear optical fiber, *Opt. Express* 21 (23) (2013) 28743–28750.
- [8] F. Parmigiani, G. Hesketh, R. Slavik, P. Horak, P. Petropoulos, D.J. Richardson, Polarization-assisted phase-sensitive processor, *J. Lightwave Technol.* 33 (6) (2015) 1166–1174.
- [9] M. Ziyadi, A. Mohajerin-Ariaei, A. Almainan, Y. Cao, M.R. Chitgarha, L. Paraschis, M. Tur, C. Langrock, M.M. Fejer, J.D. Touch, A.E. Willner, Optical channel de-aggregation of quadrature-phase-shift-keying and eight-phase-shift-keying data using mapping onto constellation axes, *Opt. Lett.* 40 (21) (2015) 4899–4902.
- [10] M. Ziyadi, A. Mohajerin Ariaei, Y. Cao, A. Almainan, A. Fallahpour, C. Bao, F. Alishahi, P. Liao, B. Shamee, L. Paraschis, M. Tur, C. Langrock, M. Fejer, J. Touch, Y. Akasaka, T. Ikeuchi, A. Willner, Tunable optical de-aggregation of a 40-Gbit/s 16-QAM signal into two 20-Gbit/s 4-PAM signals using a coherent frequency comb and nonlinear processing, in: *Conference on Lasers and Electro-Optics*, paper SM3F.5, 2016.
- [11] A. Lorences-Riesgo, T.A. Eriksson, M. Mazur, P.A. Andrekson, M. Karlsson, Quadrature decomposition of a 20 Gbaud 16-QAM signal into 2x4-PAM signals, in: *European Conference and Exhibition on Optical Communication*, paper Tu.1.E.3, 2016.
- [12] N.K. Kjoller, M. Piels, F.D. Ros, K. Dalgaard, M. Galili, L.K. Oxenlowe, 16-QAM field-quadrature decomposition using polarization-assisted phase sensitive amplification, in: *IEEE Photonics Conference*, paper WB1.5, 2016.
- [13] L. Pan, H. Wang, Y. Ji, All-optical deaggregation from 8psk to 3x4psk based on FWM in HNLF, *Appl. Opt.* 58 (5) (2019) 1246–1252.
- [14] H. Liu, H. Wang, Y. Ji, Simultaneous all-optical channel aggregation and de-aggregation for 8qam signal in elastic optical networking, *IEEE Photonics J.* 11 (1) (2019) 7900108.
- [15] Adonis Bogris, All-optical demultiplexing of 16-QAM signals into QPSK tributaries using four-level optical phase quantizers, *Opt. Lett.* 39 (7) (2014) 1775–1778.
- [16] J. Cui, G. Lu, H. Wang, Y. Ji, On-chip optical vector quadrature demultiplexer proposal for QAM de-aggregation by single bi-directional SOA-based phase-sensitive amplifier, *IEEE Access* 7 (2019) 763–772.
- [17] A. Fallahpour, M. Ziyadi, A. Mohajerin Ariaei, Y. Cao, A. Almainan, F. Alishahi, C. Bao, P. Liao, B. Shamee, L. Paraschis, M. Tur, C. Langrock, M. Fejer, J. Touch, A. Willner, Experimental demonstration of tunable optical de-aggregation of each of multiple wavelength 16-QAM channels into two 4-PAM channels, in: *Optical Fiber Communications Conference and Exhibition*, paper Th4L.6, 2017.
- [18] J.G. Proakis, M. Salehi, *Digital Communications*, fifth ed., McGraw-Hill, New York, 2008.
- [19] C. Stierstorfer, R.F.H. Fischer, Asymptotically optimal mappings for bicm with m-pam and m²-qam, *Electron. Lett.* 45 (3) (2009) 173–174.
- [20] K.O. Hill, D.C. Johnson, B.S. Kawasaki, R.I. MacDonald, Cw three-wave mixing in single-mode optical fibers, *J. Appl. Phys.* 49 (10) (1978) 5098–5106.
- [21] T. Schneider, *Nonlinear Optics in Telecommunications*, Springer-Verlag, New York, 2004.
- [22] K.P. Ho, *Phase-Modulated Optical Communication Systems*, Springer, New York, NY, 2005.
- [23] R. Essiambre, G. Kramer, P.J. Winzer, G.J. Foschini, B. Goebel, Capacity limits of optical fiber networks, *J. Lightwave Technol.* 28 (4) (2010) 662–701.
- [24] Y. Cao, M. Ziyadi, A. Almainan, A. Mohajerin-Ariaei, P. Liao, C. Bao, F. Alishahi, A. Fallahpour, B. Shamee, A.J. Willner, Y. Akasaka, T. Ikeuchi, S. Wilkinson, C. Langrock, M.M. Fejer, J. Touch, M. Tur, A.E. Willner, Pilot-tone-based self-homodyne detection using optical nonlinear wave mixing, *Opt. Lett.* 42 (9) (2017) 1840–1843.
- [25] Z. Zhang, Y. Yu, X. Zhang, Simultaneous all-optical demodulation and format conversion for multi-channel (CS)RZ-DPSK signals, *Opt. Express* 19 (13) (2011) 12427–12433.
- [26] T. Tokle, B. Zsigri, C. Peucheret, P. Jeppesen, Generation and transmission of a 160 Gbit/s polarisation multiplexed RZ-DBPSK-ASK signal, *Electron. Lett.* 41 (7) (2005) 433–434.